EUROGRAPHICS '84
K. BØ and H.A. TUCKER (Editors)
Elsevier Science Publishers B. V. (North-Holland)
© Eurographics Association, 1984

COMPUTER GRAPHICS FOR VISUALIZING SIMULATION RESULTS

Eihachiro NAKAMAE Hideo YAMASHITA Tomoyuki NISHITA
Kohichi HARADA
Electric Machinery Laboratory
Hiroshima University
Higashihiroshima 724
JAPAN

Electric & Electronic Dept.
Fukuyama University
Fukuyama 729-02
JAPAN

Computer graphics techniques for visualizing the following simulation results are developed: (1) lighting designs for different type sources such as point sources, linear sources, area sources, and polyhedron sources, (2) shaded time at arbitrary positions such as windows, walls, and even the inside of a room, (3) montages for view environment evaluation, (4) quasi-semi-transparent models for observing life generation process in anatomy, and (5) two and three dimensional magnetic fields analyzed by the finite element method.

1. INTRODUCTION

Computer graphics techniques have been being used for displaying simulation results not only of physical and chemical phenomena but also of engineering problems. Those effective display release scientists and engineers from countless output data and help their understanding of the results. Especially for researchers who study on three dimensional problems, precise observation on the output data is scarcely impossible without the help of three dimensional and/or stereographic display.
The members centered around the Electric Machinery Laboratory at Hiroshima University developed the following subjects:

(1) Illumination simulation: The realism of the shading image of a three dimensional scene is very important for lighting design. Especially shadows play an important part in shading images, and iso-lux color belts superimposed on the shading images are useful to not only designers but laymen. Most types of light sources, point sources with luminous intensity distribution characteristics, linear sources, area sources, and polyhedron sources, are dealt.

(2) Shaded time simulation: Nowadays prediction of shaded time caused by new buildings is an indispensable condition in large cities. The color belts depicting equi-shadow duration overlapped a photographic image help designers and have persuasive power to get neighbours' consent. A bird's-eye view and/or a perspective expressing the shaded time on arbitrary positions such as on windows give excellent information.

(3) Montages of a photograph and computer-generated structures: Prediction of the influence of environments on building large structures become a serious problem for designers. Zoning laws concerning the view of buildings often delay the start of construction work. The montages based on scientific methods have much more persuasive power than ones drawn by painters.

(4) Quasi-semi-transparent display for anatomy: The method of quasi-semi-transparent display with stereographics is very helpful not only to the observation of the external form and the internal organs of embryos, simultaneously, but also of any considerably complex structure.

(5) Magnetic field simulation: The output data of countless vectors distributing in two and/or three dimensional fields are unmanageable to researchers. Effective use of color information and stereographic display techniques release the researchers from that problem.

These essential points are explained.

2. ILLUMINATION SIMULATION

Half-tone representation of three-dimensional objects is one of the useful tools not only for CAD of buildings and machines but also for lighting problems. The degree of realism of the shaded image of a three-dimensional scene depends remarkably on the successful simulation of shadowing and shading effects. In order to display three-dimensional objects that look more realistic, researchers have developed techniques for simulating the properties of objects such as reflection, refraction, and transparency (e.g., Ref.[1], [2], [3]). The light sources used in those techniques, however, have been limited to parallel light sources or point light sources. Especially, in the application of computer graphics to lighting design, the calculation of shadows is very important for evaluating the arrangement of sources.

For illuminating designs, the iso-lux color belts superimposed on a photographic image gives better understanding of the illuminance distribution for not only designers, but for laymen, too.

Here it is proposed that the display methods of three-dimensional objects that are illuminated by different types of sources such as point sources, linear sources, area sources, and polyhedron sources. The advanced points of the proposed methods are as follows: 1) The use of shadow volumes formed by a convex polyhedron and a point (linear, area or polyhedron) source results in easy determination of regions of penumbrae and umbrae on faces. 2) The illuminance for point sources, linear sources, and area and polyhedron sources are calculated by taking account of the luminous intensity distribution, by using the linear integration for visible segments of the source when viewed from the calculation point, and by applying the contour integration for the visible segments of each contour line of the sources and polyhedra when viewed from the calculation point, respectively.

The method, detecting the shadow boundaries on each face prior to illuminance calculation in order to shorten the computation time, has been proposed[4],[5]. This paper makes use of the same idea, that is, shadow detection and calculation of shadow boundaries are done prior to illuminance calculation.

The conception of shadow volume for point sources and parallel sources has been proposed[6]. This idea is extended to linear(area or polyhedron) source, we defined an umbra volume and a penumbra volume formed by a convex polyhedron and each source, and then developed the calculation method of shadow boundaries on each face by using these shadow volumes as well as the method of illuminance calculation in penumbra regions.

In the algorithm described here, the following is assumed: 3-D objects are treated as sets of convex polyhedra and convex polygons. A point source has its proper luminous intensity distribution curve. The shape of a linear light source is expressed by a line segment, and the luminous characteristics are perfect diffusion and uniform brightness. The shape of an area source is a convex polygon, and the illuminating direction of the sources is only toward the positive-space. A polyhedron source is a convex polyhedron with all its faces bright.

2.1 The Outline of The Procedure

i) Input object data, viewpoints, view directions, angles of the view fields, and light sources. ii) Project the vertices of objects onto the perspective plane, and calculate the priority of visibility for the overlapped polyhedra on the perspective plane(see Ref[5]). iii) Classify the faces of each polyhedron on the positional relationship between the source and each face, and decide if the face has shadows or receives no light. iv) Obtain the volumes making umbra and

penumbra for each polyhedron (N.B., point sources have umbrae only). v) Extract the polyhedra casting shadows on the visible faces, and calculate the shadow boundaries on them. vi) Scan the perspective plane from top to bottom, that is, remove the hidden surfaces, calculate the shadow sections (umbra and penumbra) of the visible faces on each scan line, and calculate the illuminance for each point on the scan line.

2.2 Shadow Detection

In deciding whether or not one convex polyhedron casts its shadow(umbra and penumbra) on another polyhedron, we use the shadow volumes which are formed by polyhedra and light sources.

The umbra volume and the penumbra volume for an area source are determined by the following method:

We consider a shadow volume U_l which is formed by a convex polyhedron V and one vertex Q_l of a source(as shown in Fig. 1). Then, a penumbra volume is defined as the minimum convex volume surrounding U_l (l=1,2,..,m), and an umbra volume is defined as the intersection of U_l(l=1,2,..,m). In the case where the polyhedron V exists within the negative-space of the area source, V receives no light, therefore the umbra volume and penumbra volume cannot be defined. Except for this case, the umbra and penumbra volumes are defined.

In application of this same manner, the umbra and penumbra volumes for linear and polyhedron sources are determined. However, linear and polyhedron sources have no restriction for their lighting direction unlike area sources, so the penumbra and umbra volumes always exist.

The shadow exists on the face intersecting the penumbra or the umbra volume as previously mentioned.

In the first step, an intersection test between a face and a penumbra volume is executed because a penumbra volume always includes an umbra volume. If the penumbra volume and the face intersect each other, there is at least one penumbra on the face. In this case, the umbra is detected by means of the intersection test between the umbra volume and the face. The shadow boundary is obtained as the intersection region of the penumbra(or umbra) volume and the face.

2.3 Illuminance Calculation

Illuminance has two components, direct illuminance and indirect illuminance components, we, however, only discuss the direct illuminance component here.

The illuminance calculation for two conditions are required, that is, for the regions having no shadows from any polyhedra and the regions shadowed area caused by one or more polyhedra.

2.3.1 Illuminance Calculation of Unshadowed Areas

(1) Point sources

The luminous intensity of the point sources has their proper luminous intensity distribution curves, a curve representing the variation of the luminous intensity of a lamp in a plane through the light center.

The luminous intensity of each light source, I_l, generally has its own luminous intensity distribution curve; in axi-symmetric characteristic curves, it can be expressed mostly by a function of $\cos\theta$ where θ is the angle between the illumination axis and the lighting ray; e.g. $I_l(\cos\theta)=I_0(1+\cos\theta)/2$, where I_0 is the luminous intensity at $\theta=0°$.

In other cases, the luminous intensity data are given for example every ten degrees, θ_l (θ_l=0°,10°, ...,180°), and the luminous intensity in between is calculated by using linear interpolation.

The diffuse illuminance, E, at an arbitrary point P on a face S_f is

$$E = I_l(\cos\theta)\cos\alpha/r^2 \quad , \qquad (1)$$

where r is the distance between a light source Q_1 and P, α is the angle between the normal of a face S_f and the light ray from the source, and θ is the angle between the illumination axis and the light ray, the vector Q_1 P (see Fig. 2).

(2) Linear light sources

The calculation method of illuminance at an arbitrary point P on the face S_f is

described here. In Fig. 3, let W be the length of a linear source, I the illuminance intensity per unit length of the source, Q an arbitrary point on the linear source, β the angle between the vector PQ and the normal N_f of S_f, θ the angle between the vector PQ and the linear source, ℓ the distance between Q_1 and Q, and r the distance between P and Q. The illuminance E at P from a perfect diffuse linear source is given by

$$E = I\int_0^W \frac{\sin\theta}{r^2}\cos\beta d\ell \qquad (2)$$

(3) Area and polyhedron light sources

Here we assume that the light sources are composed by uniform brightness surfaces. The illuminace for area light sources can be calculated by the contour integration method for the boundary of the source(see Fig.4(a)). The illuminance calculation for polyhedron sources can be obtained by the contour

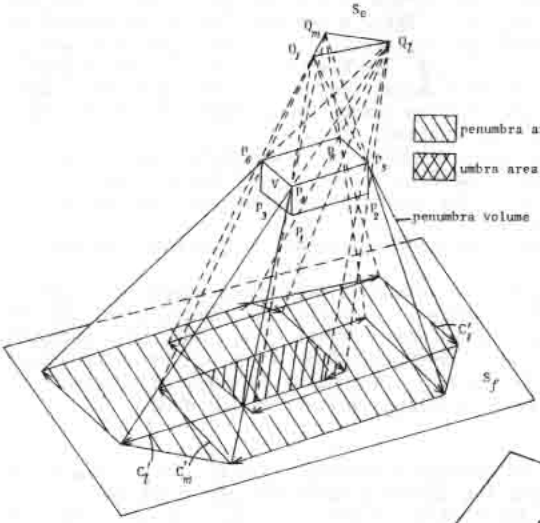

Fig. 1 Regions of umbra and penumbra for an area source.

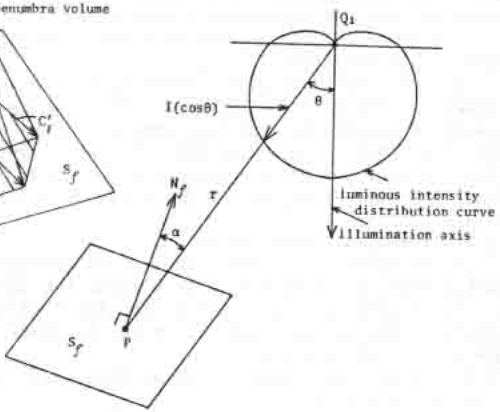

Fig. 2 Illuminance calculation for a point source.

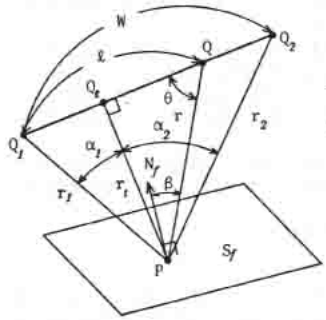

Fig. 3 Illuminance calculation for a linear source.

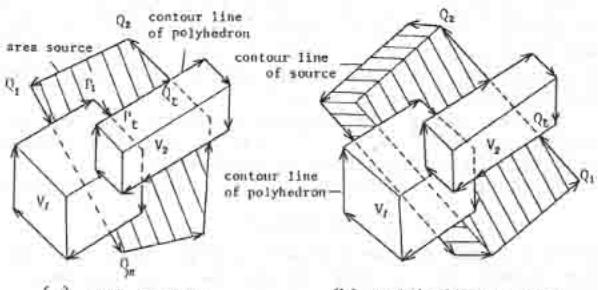

(a) area source (b) polyhedron source

Fig. 4 Illuminance calculation in penumbrae.

integration method for the contour line of the source when viewed from the calculating point (Fig. 4(b) shows the contour line of the source).

2.3.2 Illuminance Calculation in Shadow Areas

For umbrae, the illuminance calculation is simplyfied. Where we consider the shadows from many polyhedra, if the point P is included in at least one umbra, then the illuminance at P is zero.

On the other hand, the illuminance calculation in the penumbra is more complex. A penumbra area is the region in which the light from the source is partially interrupted by several polyhedra. Therefore, the illuminance at the point P must

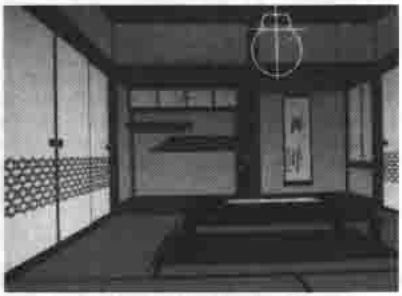

(a) point source

(b) linear source

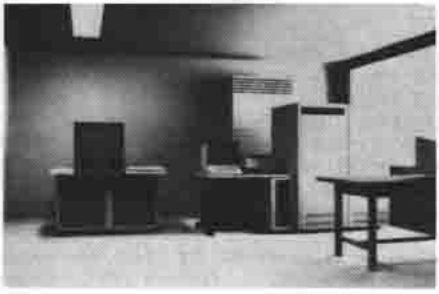

(c) area source

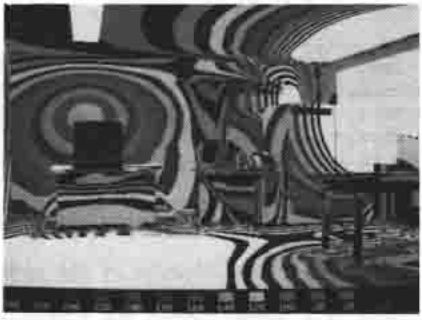

(d) illuminance distribution

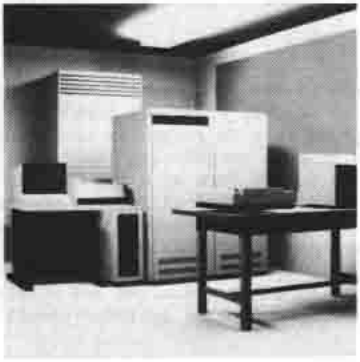

(e) polyhedron source

(f) linear source and spotlight

Fig. 5 Illumination simulation for different type sources.

be calculated by obtaining the visible parts of the light source from P. We describe only for linear, area and polyhedron sources because point sources have no penumbra.

(1) Linear light sources

The illuminance at an arbitrary point P in the penumbra is calculated by obtaining the visible parts of the linear source from P, these visible parts act to P as the new sources.

The idea of the quantitative invisibility[7] is available for determining the visible segments of the linear source. All convex polyhedra casting shadows on point P are searched, the contour lines of them observed from P are obtained, and the intersections of these contour lines and the linear source are searched. Then, the segments whose quantitative invisibility equals zero are visible.

(2) Area and polyhedron sources

The illuminance in the penumbra caused by several polyhedra and an area (or polyhedron) source can be calculated by the following procedure (first two steps are the same procedure as that of the linear sources): i) Extract the polyhedra casting penumbra on the point P. ii) Extract the contour lines of those polyhedra when viewed from P. iii) Integrate the visible segments (e.g., Q_tQ_2 in Fig. 4(a), Q_1Q_t in Fig. 4(b)) of the contour line of the source in a counter-clockwise direction. iV) Integrate the segments which exist within the contour line of the source and outside the contour lines of another polyhedra (e.g., P_1P_t in Fig. 4(a)), in a clockwise direction.

The illuminance at P is obtained by summing up the integrated values in iii) and iv) because it is equal to the integration of the closed region (shaded regions in Fig. 4).

2.4 Examples

Some examples are shown in Fig. 5. Picture (a) shows a Japanese room which is illuminated by a point light source with a luminous intensity distribution curve. Picture (b) is an example of a linear light source.

Pictures (c) and (d) are examples of lighting simulation of the interior of a room illuminated by area light sources, one of them from the ceiling lamp and the other from the window. In this room these examples were made. Picture (d) depicts the illuminance distribution of (c). The color of iso-lux belt varies in proportion to the illuminance value like a rainbow-color. The maximum value was assigned to red.

Picture (e) is an example of the room which is illuminated by two rectangular prism sources(one of them is outside the view field). Picture (f) depicts an example of a linear source and a spotlight.

As shown in these examples, it is clear that the variation of luminous intensity distribution curves and the effect of penumbrae gives much reality.

3. SHADED TIME SIMULATION

The sunshine obstruction caused by an increase in the number of multi-storied buildings and crowded areas has become one of society's serious problems in the stages of building planning. Therefore, designers have to grasp the conditions of shadows not only on the building site but also on the neighboring buildings and their sites. The equi-shadow duration curves in the form of a contour map on a plane view have been generally used. This depiction method is easy to understand for designers, but not so easy for the people in the neighborhood. A photographic image is better for everyone to understand the shadow distributions.

Here we discuss a depiction method by using a color CRT, where the color belts depicting equi-shadow duration or equi-quantity of solar radiation are overlapped on a plane view, a side view, or a perspective viewed from an arbitrary position.

3.1 The Outline of the Procedure

i) Input of the object data.

ii) Calculation of the sun path, and the sunrise and sunset time at the location of the building supposed to be built(latitude) and on a given date.

iii) Projection of the objects onto the perspective plane defined by the viewpoint and the field of view, and extraction of the visible faces of polyhedra viewed from the viewpoint.
iv) Calculation of the period of the sunshine on each visible face, where it is assumed that there are no shadows from any other polyhedra, and extraction of the polyhedra which cast shadows on each face.
v) Calculation of the shadow duration and/or the quantity of solar radiation on each point forming the visible faces; they exist on a scan line when a CRT displays the perspective image.

3.2 Calculation of Sunshine Duration

In the case when some polyhedra cast shadows on one point, the durations causing shadows often overlap as shown in Fig. 6. The sunshine duration on each point is calculated by the following method; 1) extract the polyhedra that cast shadows at least a little time on a calculation point, 2) extract contour lines of these polyhedra when viewed from the point, 3) calculate the intersection between these contour lines and the sun path, 4) extract the visible parts of the sun path(the visible parts are obtained by using the idea of quantity of invisibility[7]), 5) obtain the sunshine duration by summing up these visible segments(the shadow duration can be easily obtained by using the sunshine duration).

3.3 Calculation of the Quantity of Solar Radiation

The amount of daily solar radiation on a face having shadows is different at each point. it is obtained by the following method; the integration from beginning to end of the sunshine for every one hour is executed and the results are memorized in a look-up table. The amount of daily solar radiation at point P is obtained with the linear interpolation by means of the look-up table.

3.4 Examples

Two examples are shown in Fig.7. The pictures (a) and (b) show shadow duration on buildings and solar radiation of a room, respectively.

Since the distribution of shadow duration or the distribution of solar radiation is depicted on a perspective image viewed from an arbitrary position, one can easily grasp these distributions on arbitrary planes such as walls, windows and slopes, and furthermore the inside of a room.

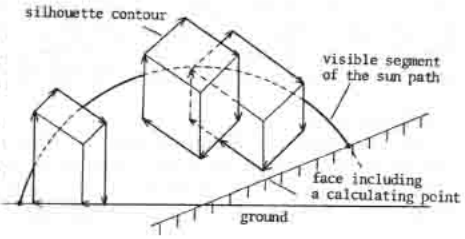

Fig. 6 The sun path viewed from a calculating point.

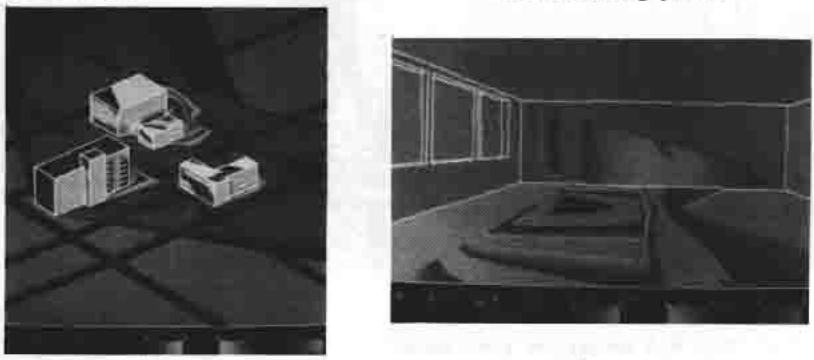

(a) (b)

Fig. 7 Distribution of shadow duration and solar radiation.

4. MONTAGE FOR ENVIRONMENT EVALUATION

A forecasting system for the influence of environment on building construction becomes very important these days.

In order to fit computer-generated structures to a photograph, the following problems should be solved: 1) anti-aliasing problems of the computer-generated structures, 2) shading considering the sun direction and weather conditions such as fog, 3) hidden surface problems of the computer-generated structures caused by the foreground, 4) geometric fitting of the computer-generated structures to the photograph. We discuss only about 2) on account of space consideration.

4.1 The Outline of the Procedure

i) Input object data and the background picture of a building site by using an optically scanned photograph. ii) Read parameters of shading and geometric information from the background picture in order to fit the computer generated structures to be built to it. iii) Display the background and superimpose the computer-generated structures. iv) Superimpose foregrounds hiding the structures.

4.2 Shading

In order to fit shading of the computer-generated structures to the background, the intensities of two surfaces of the building in the background are put out, and the ratio of direct illuminance to indirect is obtained.

Concerning fog effect, it is assumed that the color C_l (l=1,2,3; 1,2 and 3 correspond to red, green and blue) of a point P in the view field changes exponentially due to the distance r between the point P and the viewpoint. The color considering the effect of fog C_l' (l=1,2,3) is given by

$$C_l' = (1-\exp(-r/R_l))(F_l - C_l) + C_l \quad (l=1,2,3), \qquad (3)$$

where F_l is the color of the point at infinity, R_l is a constant of the color change rate. More than three points, which are similar objects, such as leaves or fields and existing at different distances from the viewpoint, are chosen. Then F_l and R_l are calculated by means of the method of least squares.

4.3 Examples

An example is shown in Fig.8. The picture (a) is an original photograph, and (b) shows a montage of a building from (a).

As shown in the example, we can get pictures which computer-generated structures fairly fit to the background.

(a) (b)

Fig. 8 A montage of a building.

5. SEMI-TRANSPARENT DISPLAY FOR AN EMBRYO'S SIMULATION

In anatomy, in order to observe the shape during the life generation process, researchers cut an embryo into slices of about seven micron thickness and make a thousand pictures from them. Then they construct a stereoimage in their mind by observing those pictures or draw a perspective for helping their observation. By means of those methods it is very difficult to observe precisely the embryo's external form and internal organs, simultaneously, even if the internal organs are a little complex. It is very helpful for observation of the embryo to construct the surface models of internal organs from the contours on each sliced section and then to display them so as to make possible the observation of the outside and the inside, simultaneously.

There are three steps for the realization of the above mentioned; input of contour lines from pictures, making surface models, and their display. For the first step we used a tablet because of the difficulty of applying the pattern recognition techniques. Concerning the second step Christiansen's algorithm[8] was improved in the following points; (1) hierachical data structure to search the connectivity of upper and lower contours, (2) branching the elements without the user's interaction, and (3) triangulation working well even if two contours drastically differ in shape.

For the last step, half-tone representation and cut models displaying an arbitrary section together with the outside are usually used. Semi-transparent display is much better for better understanding. The display, following physical property[9], is, however, not necessarily suitable for observers. Kay et al.[10] proposed to change the transparent rate for perpendicular parts to view direction higher and for parallel parts lower.

Here it's only discussed about the third step; the method of quasi-semi-transparent display and stereographic display that respond effectively and flexibly to the observer's requests.

5.1 Quasi-Semi-Transparent Display

(1) The color of each surface is given in inverse proportion to the cosine of the angle θ between the normal vector of surface and view direction. Each color element $I_{k\theta}$ (k expresses R, G, and B elements) of a face is obtained by

$$I_{k\theta} = I_{k0} / \cos(\theta - \alpha), \qquad (4)$$

where I_{k0} is a color of k when θ and α are equal to zero and α a parameter to change the phase of brightness of surfaces. This technique helps to emphasize semi-transparency and to make it easy to grasp the shapes of both the inside and the outside, simultaneously.

(2) The brightness of a face is every time made t_i times when there is the element i in front of it, where t_i is transparent rate of the element i . The transparent rate t_i is a variable corresponding to one's demands. If t_i is equal to zero, all faces locating behind the ith face are completely hidden.

(3) The brightness of every face decreases in proportion to the square of the distance between the view point and a face. Therefore, the final color element I_k of the face is

$$I_k = K * I_{k\theta} / r^2 * \Pi t_i \quad (k = R, G, B), \qquad (5)$$

where K is a correction facter and r the distance between a standard point chosen by observers and the face.

5.2 Stereographic Display

A perspective view is usually useful for understanding three dimensional objects, but it's only for when people already have some concept of them. It doesn't work well for unknown objects especially for semi-transparent objects because originally the perspectives only give two dimensional information. Stereographic display gives observers tremendously real images of semi-

transparent objects.

5.3 Examples

Here a section of a mouse's head embryo is used for examples. Fig. 9(a) shows a stereographic image. Fig. 9(b) is an example of changing phase α for observation of the front faces more precisely. An article shown in Fig.10 is a sort of engineer's diversion.

Fig. 9(a) Semi-transparent stereographic display of mouse's embryo.

Fig. 9(b) Changing phase of brightness.

Fig. 10 Semi-transparented apples.

6. MAGNETIC FIELD SIMULATION[16]

The finite element method for electric and magnetic fields is very popular because of its powerful numerical techniques. Since the output from the finite element analyses (F.E.A.) usually makes a pile of numerical data, it is very important to display them intelligibly and accurately in order to assist analysts in understanding and evaluating the results. Three post-processing methods in the F.E.A. using a multi-color pen plotter or a color CRT are developed: (1) Depiction of magnetic flux lines in two or three dimensional fields by using a multi-color pen plotter, (2) Depiction of magnetic flux density distribution with flux lines in two dimensional fields by using a color CRT, (3) Depiction of error distribution by using a color CRT.
Here, the methods for (1) and (2) are discussed because of space limitation. The depictions in (1) and (2) make it possible to display the magnitude and direction of vectors and their loci simultaneously; here (1) is also available to the stereographic display of the results of the three dimensional F.E.A.

These methods are also applied not only to magnetic field problems but also to every static physical phenomena handling distributed vectors in two or three dimensional fields; for example, electric field problems (electric force lines and

intensity of the electric field), thermal problems (temperature gradient and heat flow), and flow problems (flow lines and flow rate). Furthermore, these methods are available not only to computed results but also to measured values by means of the interpolation technique.

6.1 Depiction of magnetic flux lines in two or three dimensional fields by using a multi-color pen plotter

The depicting methods using an X-Y plotter for representing the results of the F.E.A., which are frequently used at present, are the following;

(1) Drawing the results of the two dimensional or axi-symmetrical F.E.A.,
(A) drawing of magnetic flux lines by means of contour lines[11], and
(B) drawing of magnetic flux density vectors[12],
(2) Drawing the results of the three dimensional F.E.A.,
(C) drawing of magnetic flux density vectors at some specified points on a chosen plane[13], and
(D) depicting a perspective of flux lines on some chosen cross sections[14].

Method A only depicts the loci of the magnetic flux density vectors, so even in the two dimensional cases the analysts have to infer the magnitudes of the magnetic flux density from the distance between each of the two flux lines. In axi-symmetrical cases, the magnetic flux density of an arbitrary observation point is the result of dividing the distance between the two flux lines by the radius. Therefore, it is almost impossible for the analysts to estimate the magnetic flux density distribution from the depiction of method A in the axi-symmetrical case. This difficulty is clearly shown in the section 6.3.

Method B gives the magnitude and direction of vectors, but it does not give any loci of the vectors. Furthermore, the analysts need to measure each vector length in order to get the accurate values when necessary because of their analog quantities.

Method C gives the magnitude and direction of magnetic flux density vectors at arbitrary points on a sampled plane in a three dimensional space: two arrows are depicted, one of them shows the direction of a magnetic flux density vector by projecting the arrow on the plane and the other arrow scaled in proportion to the magnitude of magnetic flux density is drawn at a right angle to the former vector. Using this method, the direction of the magnetic flux density can not be accurately estimated. In addition, the observation of the loci of the magnetic flux density vectors is impossible.

In Method D, the real flux lines are drawn only on the symmetrical cross sections in a model. It means that this method is not useful for depicting the results of the three dimensional F.E.A.

To overcome the weak points mentioned above the following methods are discussed; the magnitude, direction, and loci of magnetic flux density vectors in two or three dimensional fields are simultaneously depicted by using color display. Each magnetic flux line is divided into some parts with different colors according to the magnitude of magnetic flux density. The line also has an arrow to show its direction. A multi-color pen plotter which was just recently put on the market with comparatively low cost is available. The special features of this method are as follows:

(1) Analysts can numerically grasp the magnitude of magnetic flux density from the various colors of the lines.
(2) By using stereographic techniques to three dimensional magnetic flux lines[15],[16], analysts can intuitively comprehend both the behavior of the magnetic flux lines in three dimensional space and the magnetic flux density value.
(3) From the arrow displayed on each line, we can understand its direction at a glance.

6.2. Depiction of magnetic flux density distribution with magnetic flux lines in a two dimensional field by using a color CRT

A raster scaning type color CRT gives much more information than a color plotter: the CRT has potential ability to display the magnetic flux density

distribution all over the required area in a two dimensional or axi-symmetrical field. The area where the analyst concentrates his attention usually has a high magnetic flux density; if the magnetic flux lines are drawn in the area by using the method mentioned in the former section, there is no problem for observing the F.E.A. results in almost all cases. However, if not only the magnetic flux lines but also the magnetic flux density distribution are displayed on the CRT, it is more convenient for investigating the results of the F.E.A. because one can grasp at a glance and estimate the behavior of the magnetic field.

Here, the following quasi-color displaying method is described: the display of magnetic flux density distribution is processed with high speed by means of dividing each second order triangular element into four small triangles. That is, it is assumed that the magnitude of the magnetic flux density is approximated to linear in each small triangle. The small triangle is divided into several elements. Each element is assigned a color corresponding to the magnitude of its magnetic flux density. Then, the magnetic flux distribution, painted by color, appears on the CRT. After the process mentioned above is completed, the magnetic flux lines are lapped over the magnetic flux distribution.

6.3 Examples

The depiction methods described above are applied to the models shown in Figs. 11 (a) and (b). Note that in these models the shapes of the cross sections of the coils and irons in every quadrant are exactly the same. Figs. 12 and 13 show the color depictions of the magnetic flux lines and the magnetic flux density distribution by the methods described in the sections 6.1 and 6.2, respectively, where the color information in these figures cannot be shown because of monochrome print.

In Figs. 13 (a) and (b), the color scale used here has ten color levels and five brightness levels on each color; it is suitable to numerically grasp the magnitude of magnetic flux density.

The flux line distributions in Figs. 12 (a) and (b) are almost the same, but the magnetic flux density distribution in Figs. 13 (a) and (b) are quite different. When the model is an axi-symmetric one as shown in Fig. 11 (b), it would be difficult to estimate the magnetic flux density distribution from only the map of the magnetic flux lines, even if one tries to do this with the observation of the distance of the two magnetic flux lines. By using the method described here, these drowbacks can be defeated smartly; we can visually grasp the magnitude of the magnetic flux density and the behavior of the magnetic flux lines simultaneously, even in an axi-symmetrical model.

The method in the section 6.1 was also applied to the results of three dimensional F.E.A. of an air-gap reactor. Fig. 14 shows the color graph of this example. From two color graphs in Fig. 14, we can observe the behavior of the three dimensional magnetic field as a stereoimage.

ACKNOWLEGEMENT

The authors are grateful to Dr. Yasuda and Dr. Sato, Anatomy Laboratory, Medical Department, Hiroshima University, for their eager discussion and the offering of data of the mouse embryo. Particular thanks are due to the members of Electric Machinery Laboratory for their support.

REFERENCES

[1] Bui-Tuong, Phong, Illumination for Computer-Generated Pictures, Comm. ACM 18 6(1975) 311-317.

[2] Whitted,T., An Improved Illumination Model for Shaded Display, Comm. ACM 23 6(1980) 343-349.

[3] Cook,R.L. and Trrance,K.E., A Reflectance Model for Computer Graphics, acm Trans. on Graphics 1 1(1982) 7-24.

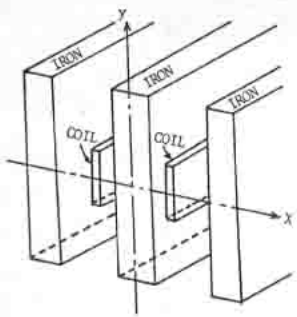

(a) Model I (Two Dimensional Field)

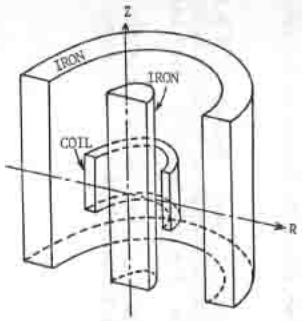

(b) Model II (Axi-symmetrical Field)

Fig. 11 Models applied the F.E.A.

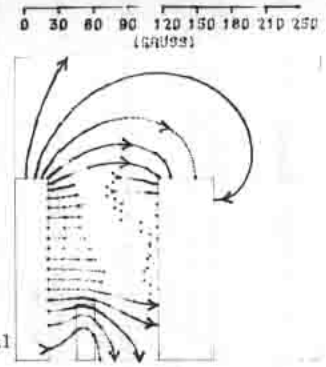

(a) Model I

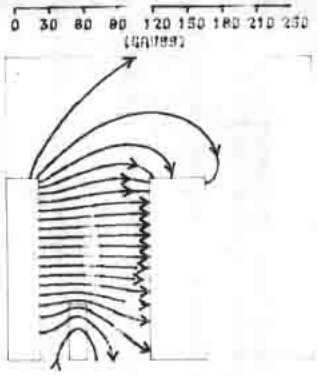

(b) Model II

Fig. 12 Color depiction of the magnetic flux lines.

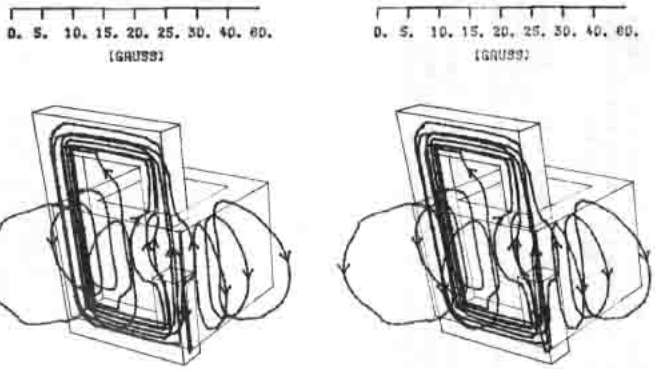

Fig. 14 Color depiction of the magnetic flux lines in three dimensional field.

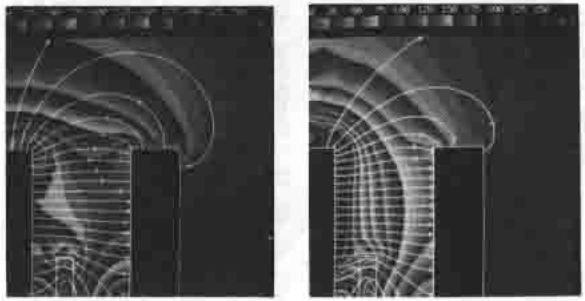

(a) Model I (b) Model II

Fig. 13 Color deliction of the magnetic flux density distribution.

[4] Atherton,P. , K. Weiler, and Greenberg,D., Polygon Shadow Generation, Computer Graphics 12 3(1973) 275-281.

[5] Nishita,T. and Nakamae,E., An Algorithm for Half-Toned Representation of Three Dimensional Objects, Information Processing Society of Japan 14 (1974) 93-99.

[6] Crow,F.C., Shadow Algorithms for Computer Graphics, Computer Graphics 11 2(1977) 242.

[7] Appel,A., The Notion of Quantitative Invisibility and the Machine Rendering of Solids, Proc. ACM, Na. Conf. (1967) 387.

[8] Christiansen,H.N. et al., Conversion of Complex Contour Line Definitions into Polygonal Element Mosaics, Proc. acm SIGGRAPH'78 (1978) 187-192.

[9] Sunguroff,A. et al., Computer Generated Images for Medical Applications, Proc. acm SIGGRAPH'78 (1978) 196-202.

[10] Kay,D.S. et al., Transparency for Computer Synthesized Images, Proc. acm SIGGRAPH'79 (1979) 158-164.

[11] Yamashita,H., Nakata,N., and Nakamae,E., Expression of results of finite element analysis using second order triangular elements, Trans. of Information Processing Society of Japan, 22, 2(1981) 106-113.

[12] Bossavit,A., A mixed FEM-BIEM method to solve 3-D eddy-current problems, IEEE Trans. on Magnetics MAG-18 2(1982) 431-435.

[13] Fuller,A.J.B. and Santos,M.L.X., Computer generated display of 3-D vector fields, Computer Aided Design 12 2(1980) 61-66.

[14] Chari,M.V.K., Konrad,A., Palmo,M.A., and D'Angelo,J., Three-Dimensional Vector Potential Analysis for Machine Field Problems,IEEE Trans. on Magnetics MAG-18 2(1982) 436-446.

[15] Yamashita,H., Harada,K., Nakamae,E., Itano,J., and Hammam, M.S.A.A., Stereographic display on three dimensional magnetic fields of electromagnetic machines, IEEE Trans. on Power App. and Systems PAS-100 11(1981) 4692-4697.

[16] Nakamae,E., Yamashita,H., Kawano,N., and Nakano,S., Color Computer Grahics in Magnetic Field Analysis by Means of The Finite Element Method, Computers & Graphics 7 3-4(1983) 295-306.